Cellular and Molecular Biology
E-ISSN : 1165-158X / P-ISSN : 0145-5680
www.cellmolbiol.org

Inhibiting MiR-320a promotes myocardial apoptosis in myocardial infarction rats through activating VEGF pathway

Yong Liu[#], Ting Wang[#], Hongmei Lai, Jingyi Shen, Fangming Gao[*]

Heart and Panvascular Diagnosis and Treatment Center, 91 Tianchi Road, Tianshan District, Urumqi, Xinjiang, China

[#] Yong Liu and Ting Wang contributed equally to this work.

ARTICLE INFO

Original paper

Article history:
Received: June 08, 2023
Accepted: September 07, 2023
Published: November 30, 2023

Keywords:

Myocardial infarction, miR-320a, vascular endothelial growth factor, apoptosis

ABSTRACT

To detect the expressions of vascular endothelial growth factor (VEGF) and micro ribonucleic acid (miR)-320a in myocardial cells of rats with myocardial infarction (MI), and to study the detailed mechanism of the role of miR-320a in myocardial apoptosis in MI rats. The Sprague-Dawley rat model of MI was established, and the rats were randomly divided into a control group (n=8), recombinant adeno-associated virus (rAAV)-miR-320a group (n=8) and rAAV-miR-320a TuDs group (n=8). The corresponding rAAV (1×10^{11} virion-like particles) was intravenously injected. At 2 weeks after the injection of rAAV, all rats were euthanatized, and the organs were collected, frozen in liquid nitrogen and stored at -80°C for further experiments. The total RNA and total protein were extracted from heart tissues, and the expression levels of rAAV-miR-320a and rAAV-miR-320aTuDs in heart tissues were determined *via* reverse transcription-polymerase chain reaction (RT-PCR). Moreover, RT-PCR and Western blotting were performed to detect the mRNA and protein expressions in heart tissues, respectively. At the same time, myocardial apoptosis was evaluated through flow cytometry. After treatment with miR-320a TuDs, the mRNA and protein expressions of VEGF in heart tissues in MI were significantly increased ($P<0.05$). The results of flow cytometry showed that miR-320a TuDs intervention could promote myocardial apoptosis in MI ($P<0.05$). In addition, the results of Western blotting revealed that miR-320a TuDs could facilitate the activation of the VEGF signaling pathway in heart tissues in MI ($P<0.05$). Inhibiting miR-320a can promote myocardial apoptosis through activating the VEGF signaling pathway in myocardial cells in MI.

Doi: http://dx.doi.org/10.14715/cmb/2023.69.12.27

Introduction

Coronary artery disease, also known as ischemic heart disease (IHD), has been the major cause of death and disability around the world in the past 15 years (1-3). Myocardial infarction (MI) refers to the acute coronary occlusion caused by coronary atherosclerosis, plaque rupture and thrombosis. Persistent myocardial ischemia can eventually result in irreversible myocardial injury, and regeneration is difficult for damaged myocardial cells. As a result, the myocardium supplied by the occluded coronary artery becomes disabled and even endangers life (4,5). Therefore, restoring blood supply is critical for the successful treatment of IHD. It is reported that a large number of proteins protect the host from myocardial ischemia and reperfusion injury through regulating myocardial apoptosis and inflammation. Studies have shown that early myocardial apoptosis may increase the incidence of MI (4-6).

Vascular endothelial growth factor (VEGF) is considered the most important cytokine promoting endothelial cell growth, which plays a vital role in maintaining the stability of the vascular endothelial structure, facilitating endothelial cell proliferation and regeneration, and inhibiting apoptosis. According to previous studies, VEGF may help the survival and proliferation of endothelial cells and protect cells from apoptosis through inducing the expressions of anti-apoptosis and antioxidant proteins (7-10). VEGF can directly induce the phosphorylation of VEGF receptor 2, thereby activating the downstream signaling molecules in the apoptotic pathway, whose mechanism is that Apatinib reduces the VEGF-mediated PI3K/Akt signal transduction and increases apoptosis in a dose-dependent manner.

Micro ribonucleic acids (miRNAs) are a kind of small non-coding RNAs that regulate the gene expression at the post-transcriptional level through binding to their target messenger RNAs (mRNAs) (11-13). There is increasingly more evidence that miRNAs play key roles in a variety of physiological/pathological processes. It is speculated that a single miRNA can regulate many processes through multiple targets. Some miRNAs have tissue-enriched or even tissue-restricted features, which can control the gene expression in some organs or tissues (14-17). More importantly, miRNAs may become promising therapeutic targets for diseases. In the present study, the effect of miR-320a on myocardial apoptosis after MI and the expression of VEGF were explored, so as to clarify the mechanism of action of miR-320a in myocardial apoptosis in rats.

* Corresponding author. Email: gaofangming@souhou.com

Materials and Methods

Laboratory animals

Male Wistar rats weighing 225-250 g were purchased from the Laboratory Animal Center of South China University of Technology, and they were fed with drinking water and rodent feed in separate cages under the natural light and controlled humidity/temperature. This study was approved by the Animal Ethics Committee of Heart and Panvascular Diagnosis and Treatment Center Animal Center.

Laboratory reagents

Rabbit anti-VEGF, B-cell lymphoma-2 (Bcl-2) and Bcl-2 associated X protein (Bax) polyclonal antibodies were obtained from ABclonal Biotech (Cambridge, MA, USA), the polyvinylidene fluoride (PVDF) membranes from Bio-Rad (Hercules, CA, USA), horseradish peroxidase (HRP)-conjugated secondary antibodies and enhanced chemiluminescence reagents from Pierce Biotech (Rockford, IL, USA), the miR-320a mimics/inhibitors, negative control and miRNA primers from RiboBio (Guangzhou, China), the endotoxin-free plasmid purification kit from Tiangen (Beijing, China), the mRNA primers from BGI Tech (Shenzhen, China), and the DNA ladder and pre-stained protein markers from Thermo Fisher Scientific (Waltham, MA, USA).

Experimental methods

Construction of plasmids and preparation of recombinant adeno-associated virus (rAAV)

To control the expression of miR-320a in vivo, the type 9 rAAV system was used. The oligonucleotide and its complementary sequences were synthesized by BGI Tech (Shenzhen, China), annealed and ligated to the rAAV vectors. The miR-320a(5'-AGCTTTCGCCCTCTCAACCCAGCTTTTTTCAAGAGAAAAAGCTGGGTTGAGAGGGCGACCGC-3) and miR-320a TuDs(5'-GACGGCGCTAGGATCATCAACTCGCCCTCTCAAATCTCCCAGCTTTTCAAGTATTCTGGTCACAGAATACAACTCGCCCTCTCAAATCTCCCAGCTTTTCAAGATGATCCTAGCGCCGTCTTTTTT-3') designed were packaged with the rAAV, followed by purification as previously described.

Grouping and modeling

The rats were anesthetized with an intraperitoneal injection of Zoletil (30 mg/kg) and connected to a ventilator for surgery. Briefly, the skin was depilated and carefully cut open to expose the heart. Then the anterior descending coronary artery was ligated using the 3-0 silk thread at 3 mm away from the left auricle. The heart was placed in the thoracic cavity for 3-4 min, and the wound was closed using the suture line layer by layer. The rats were supported by the ventilator until the spontaneous respiratory function was restored. The skin around the suture line was wiped with 70% ethanol, and the rats were placed in clean separate cages for resuscitation. During the first 4 d, acetaminophen (50 mg/kg) was administrated to limit the postoperative pain, and the wound care needed was given to avoid infection. The rats were randomly divided into a control group (n=8), rAAV-miR-320a group (n=8) and rAAV-miR-320a TuDs group (n=8). The corresponding rAAV (1×10^{11} virion-like particles) was intravenously injected. At 2 weeks after the injection of rAAV, all rats were euthanatized, and the organs were collected, frozen in liquid nitrogen and stored at -80°C for further experiments or fixed with formalin for histological analysis.

Echocardiography

The cardiac function and structure were evaluated using the high-frequency ultrasound system (Vevo2100). Briefly, the rats were anesthetized with 5% isoflurane using the breathing apparatus, and the left chest was carefully scanned for two-dimensional echocardiographic measurement, including left ventricular internal diameter at end-diastole (LVIDd), left ventricular internal diameter at end-systole (LVIDs), left ventricular ejection fraction (LVEF) and left ventricular fractional shortening (LVFS).

Detection of apoptosis via flow cytometry

A tissue block (3 mm^3) was taken from the frozen sample of the left ventricle, and 3 mL of digestion buffer was added and mixed evenly in a water bath at 36°C for 80 min. After the supernatant was discarded, 2 mL of digestion buffer was added for digestion for another 30 min, followed by natural sedimentation. Then the cell suspension was collected, and the precipitated tissue block was restored for 1 h. 50 g of liquid digested twice was taken and centrifuged for 2 min, the supernatant was discarded, and the liquid was added with fluorescein isothiocyanate (FITC) and mixed with the labeled Annexin V, followed by incubation at room temperature for 10 min, further centrifugation and washing with PBS. The cells were resuspended with binding buffer (1×), added with 1 μg/L inorganic phosphate in the dark and placed at room temperature for 30 min, followed by filtration through the nylon mesh (40 μm). The apoptosis rate was measured using fluorescence-activated cell sorting. The cell cycle was analyzed using the data acquisition software CellQuest and the DNA analysis software ModFit LT.

Analysis of related protein expression using Western blotting

The total protein was extracted using radioimmunoprecipitation assay (RIPA) lysis buffer (Beyotime, Shanghai, China), and the protein concentration was determined using the bicinchoninic acid (BCA) kit (Pierce, Rockford, IL, USA). The 10% sodium dodecyl sulfate (SDS) separation gel and spacer gel were prepared. The cell samples were mixed with the sample buffer, heated in boiling water at 100°C for 5 min, subjected to an ice bath and centrifugation, and added into each electrophoresis lane using the pipette for electrophoretic separation of the same amount of proteins. Then the proteins in the gel were transferred onto PVDF membranes, sealed with 5% dry skim milk at 4°C overnight, and incubated with the diluted primary antibodies of VEGF (1:1000), Bcl-2 (1:1000), Bax (1:1000) and GAPDH (1:2500) overnight, washed with phosphate buffered saline (PBS) for 3 times (5 min/time), incubated again with the commercially available HRP-conjugated rabbit anti-immunoglobulin G polyclonal antibody (1:200) at 37°C for 1 h and washed again with PBS for 3 times (5 min/time), followed by color development using ECL solution (ECL808-25, Biromiga, CA, USA) at room temperature for 1 min. Finally, the excess liquid was removed, the proteins were covered with a protective film, and the protein level was observed using the X-ray machine

Table 1. Primer sequences.

Gene	Primer sequence
VEGF	F: 5′-AGCCAGAAA ATCACTGTGAGCC-3′
	R: 5′-TTTAACTCAAGCTGCCTCGCC-3′
Bcl-2	F: 5′-TGGACAACATCGCTCTGTGGA-3′
	R: 5′-TCAAACAGAGGTCGCATGCTG-3′
Bax	F: 5′-GGTTTCATCCAGGATCGAGCA-3′
	R: 5′-CGTCAGCAATCATCCTCTGCA-3′
β-actin	F: 5′-ATGAAGATCCTGACCGAGCGTG-3′
	R: 5′-CTTGCTGATCCACATCTGCTGG-3′

(36209ES01, Qian Chen Biological Technology Co., Ltd., Shanghai, China).

Detection of related gene expression via quantitative reverse transcription-polymerase chain reaction (qRT-PCR)

The total RNA was extracted using a TRIzol reagent (Invitrogen, Carlsbad, CA, USA). The myocardial cells were added with 1 mL of TRIzol reagent, vortexed and mixed with 200 μL of chloroform, followed by centrifugation at 12,000 g and 4°C for 10 min. Then the supernatant was transferred into a new tube containing 500 μL of isopropanol and centrifuged again at 12,000 g and 4°C for 10 min, and the supernatant was discarded. The precipitate was washed with 75% ethanol and centrifuged at 12,000 g and 4°C for 10 min, and the RNA precipitate was taken and air-dried. Finally, free ddH_2O was added to dissolve the RNA precipitate. The RNA concentration was measured using a spectrophotometer, and the optical density $(OD)_{260}/OD_{280}$ ratio and total RNA mass were analyzed. Then RNA was transcribed into complementary deoxyribonucleic acid (cDNA) using the TaKaRa kit (Dalian, Liaoning, China). The primers for β-actin, VEGF, Bax and Bcl-2 were designed and synthesized by TaKaRa (Dalian, Liaoning, China) (Table 1). Then qRT-PCR was performed using the ABI 7500 Real-Time PCR System (ABI, Foster City, CA, USA) under the following conditions: pre-denaturation at 95°C for 5 min, and 40 cycles of denaturation at 95°C for 10 s, annealing at 60°C for 20 s and extension at 60°C for 30 s. The qPCR system (20 μL) included 10 μL of SYBR Premix Ex Taq™ II, 0.8 μL of PCR forward primers (10 μM), 0.8 μL of PCR stock primers (10 μM), 0.4 μL of ROX Reference Dye, 2.0 μL of cDNA template, and 6.0 μL of sterile distilled water. β-actin was used as an internal reference for VEGF, Bax and Bcl-2. This experiment was repeated for 3 times.

Hematoxylin-eosin (HE) staining

The frozen tissues (n=3 per group) were taken, fixed with 10% paraformaldehyde and sliced into 4 μm-thick paraffin sections. The sections were placed in xylene I for 10 min and xylene II for 10 min, incubated with the mixture of xylene and ethanol (1:1), and dehydrated with 100%, 95%, 85%, 70% and 50% alcohol for 5 min, and washed with distilled water for 3 min. The sections were taken out of the distilled water, stained with hematoxylin for 5-10 min and washed with running water to remove the residual hematoxylin. Then the sections were placed in 1% hydrochloric acid-ethanol for reaction for 2-10 min until they turned red, washed with running water and observed under a light microscope. After the sections were washed until they returned to blue, they were dehydrated with 50%, 70% and 85% alcohol for 2 min, re-stained with 1% eosin-ethanol mixture for 1-3 min and washed again, followed by dehydration with 95% ethanol for 1 min and 100% ethanol for 5 min. Then the sections were reacted in the mixture of xylene and ethanol (1:1), placed in xylene I for 5 min and xylene II for 5 min, sealed with neutral balsam and stored. Finally, the pathological changes in myocardial tissues were observed under the light microscope.

Detection of apoptosis using TUNEL/DAPI immunofluorescence assay

The myocardial tissues obtained (n=3 per group) were immediately fixed with 4% paraformaldehyde, dehydrated, embedded in paraffin and sliced into 4 μm-thick sections using a microtome. The sections were placed on the glass slide, baked in an oven at 65°C for 10 min, dehydrated with xylene and ethanol, and washed with PBS 3 times (5 min/time). Then the apoptosis after treatment was detected using the TUNEL/DAPI immunofluorescence assay kit (Beyotime Institute of Biotechnology, Shanghai, China), and the number of nuclei was assessed *via* 4',6-diamidino-2-phenylindole (DAPI) (Sigma-Aldrich, St. Louis, MO, USA) staining. The TUNEL-positive cells were observed under a fluorescence microscope (400×, Leica, Wetzlar, Germany), and the area of TUNEL- and DAPI-positive staining was determined using ImageJ software (NIH, Bethesda, MD, USA).

Statistical analysis

Statistical Product and Service Solutions (SPSS) 21.0 software (IBM, Armonk, NY, USA) was used for data analysis. All experiments were repeated 3 times in each group. Differences between two groups were analyzed by using the Student's t-test. Comparison between multiple groups was done using a One-way ANOVA test followed by Post Hoc Test (Least Significant Difference). $P<0.05$ suggested the statistically significant difference.

Results

Effect of miR-320a on cardiac function

The expression of mature miR-320a in rats was controlled using rAAV-miR-320a. First, it was confirmed *via* PCR that rAAV-miR-320a treatment increased the expression of miR-320a, while rAAV-miR-320a TuDs reduced the expression of miR-320a in heart tissues (Figure 1A). Next, echocardiography was performed to detect the effect of miR-320a on cardiac function. Interestingly, it

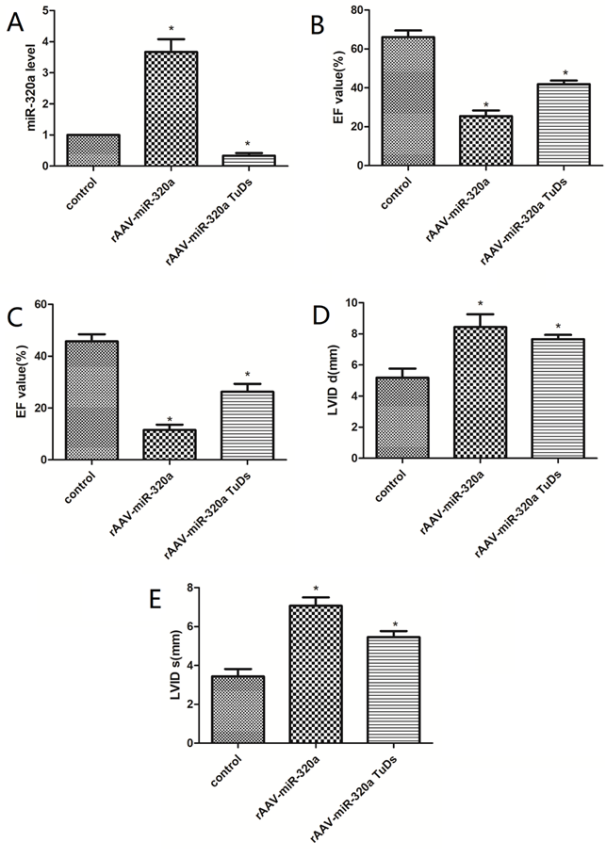

Figure 1. (A) Expression of miR-320a in heart tissues detected via PCR. (B, C, D & E) Echocardiography for rats under different treatments. $^{*}P<0.05$ *vs.* control group.

was found that rAAV-miR-320a TuDs improved cardiac dysfunction, while rAAV-miR-320a aggravated cardiac dysfunction (Figure 1A). Both EF and FS in the rAAV-miR-320a TuDs group were also significantly improved compared with those in the control group (Figure 1B & 1C), and both LVIDd and LVIDs declined in rAAV-miR-320a TuDs group (Figure 1D & 1E).

Effect of miR-320a on myocardial apoptosis

Compared with that in the control group and rAAV-miR-320a group, the apoptosis rate in the rAAV-miR-320a TuDs group was increased ($P<0.05$), indicating that inhibiting miR-320a activates the VEGF signaling pathway and increases myocardial apoptosis (Figure 2).

Inhibiting miR-320a could increase the protein levels of VEGF and Bax, and decrease the protein level of Bcl-2

Compared with the control group and the rAAV-miR-320a group, the rAAV-miR-320a TuDs group had increased protein levels of VEGF and Bax ($P<0.05$), but a decreased protein level of Bcl-2. The above results demonstrate that miR-320a TuDs raise the protein levels of VEGF and Bax, resulting in increased protein levels of the signaling pathway and apoptosis-related genes (Figure 3).

Inhibiting miR-320a could increase the mRNA levels of VEGF and Bax, and decrease the mRNA level of Bcl-2

Compared with the control group and the rAAV-miR-320a group, the rAAV-miR-320a TuDs group had increased mRNA expressions of VEGF and Bax, but a decreased mRNA expression of Bcl-2 ($P<0.05$). It can be seen that miR-320a TuDs can raise the mRNA expressions of VEGF and Bax, and lower the mRNA expression of Bcl-2, thereby increasing the mRNA expressions of signaling pathway and apoptosis-related genes (Figure 4).

Inhibiting miR-320a remarkably enhanced myocardial apoptosis

The morphology of myocardial tissues was observed using HE staining. In the rAAV-miR-320a group, myocardial cells were seriously damaged, necrotic tissues were infiltrated by many neutrophilic granulocytes, and surviving myocardial cells were distributed disorderly compared with the control group. However, the myocardial tissues in the rAAV-miR-320a TuDs group were improved. The number of apoptotic myocardial cells in the rAAV-miR-320a TuDs group was remarkably larger than that in the control group and rAAV-miR-320a group ($P<0.05$) (Figure 5).

Discussion

MI occurs in the case of coronary artery occlusion in patients, leading to myocardial hypoxia, and death of

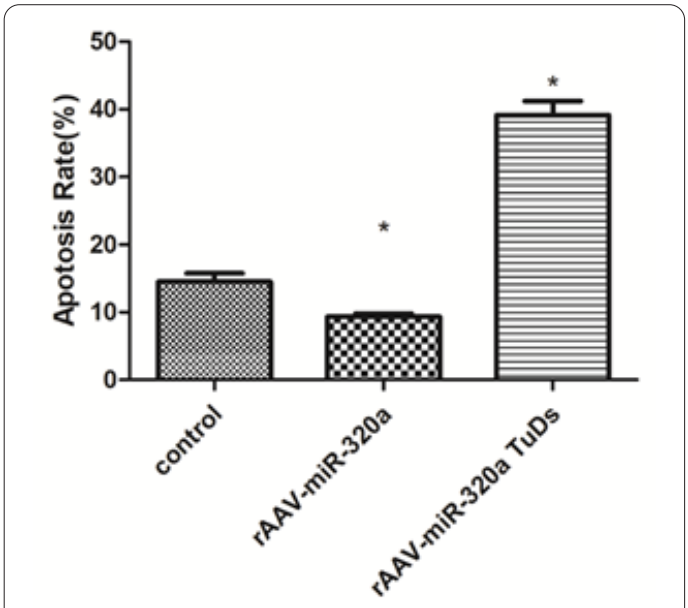

Figure 2. Overexpression of miR-320a reduces myocardial apoptosis while inhibiting miR-320a expression increases myocardial apoptosis. $^{*}P<0.05$ *vs.* control group.

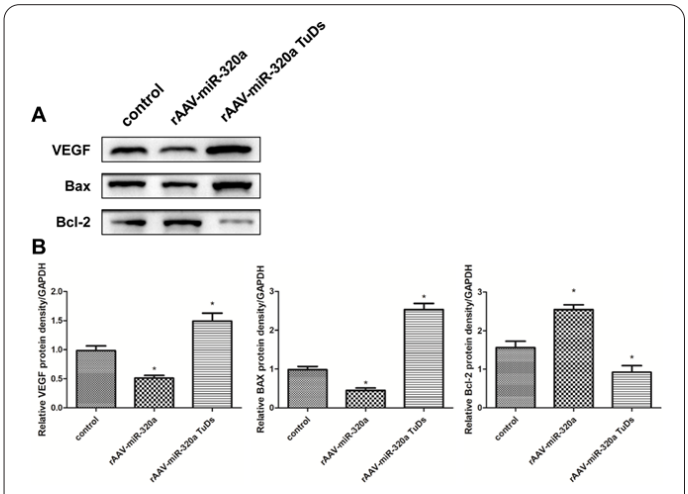

Figure 3. Protein levels of VEGF, Bax and Bcl-2 in myocardial cells. $^{*}P<0.05$ *vs.* control group.

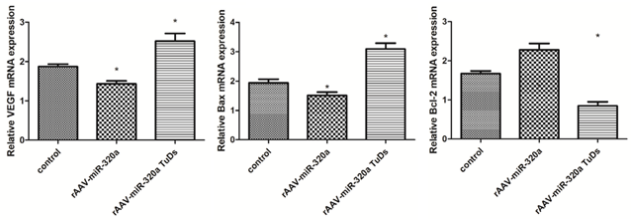

Figure 4. mRNA levels of VEGF, Bax and Bcl-2 in myocardial cells. $^{*}P<0.05$ *vs.* control group.

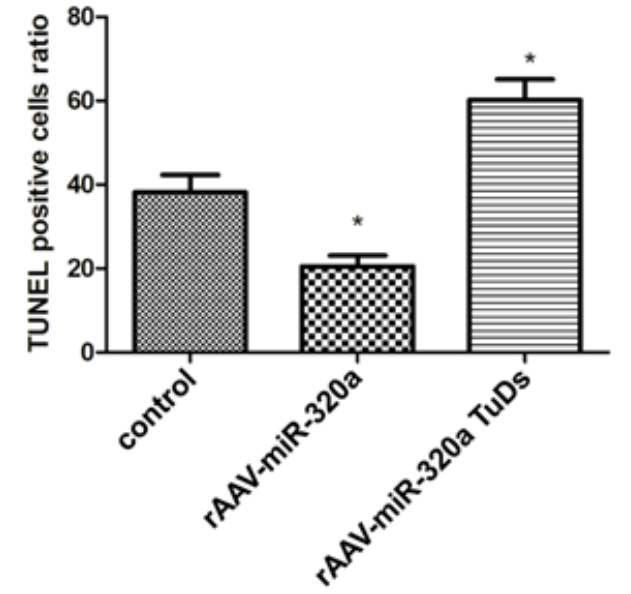

Figure 5. Evaluation of myocardial apoptosis. The ratio of TUNEL-positive cells to DAPI-positive cells. $^{*}P<0.05$ *vs.* control group.

myocardial and non-myocardial cells. Then left ventricular remodeling or maladaptation and even heart failure will be induced (1). MI has a high mortality rate in the world, which is one of the most important factors for disability globally (2). MI can also induce a sterile inflammatory response and lead to poor ventricular remodeling (3). Many factors contribute to the development of MI, including genetic and some controllable factors, such as age, systolic blood pressure, hypertension, cholesterol, diabetes, smoking history and abnormal body mass index (4,5). The mortality rate of acute MI declines with the timely revascularization of ischemic myocardium, but its long-term mortality rate remains high (6). Therefore, new therapeutic methods must be found to reduce the death and disability caused by MI.

Apoptosis is a kind of programmed cell death characterized by cell membrane blebbing, cell shrinkage, nuclear fragmentation, chromatin condensation and chromosomal DNA fragmentation. It is reported in many clinical and subclinical studies that the apoptotic pathway is activated in MI, and it has been found that 11 Bcl-2 family members play key roles in promoting or inhibiting the intrinsic apoptotic pathway triggered by mitochondrial dysfunction. Therefore, the balance between pro-apoptotic and anti-apoptotic factors can determine the cell fate. Bax and Bcl-2 are major members of the Bcl-2 family, the former of which responds to different cellular stress through the outer mitochondrial membrane to promote cell death, but the latter of which prevents apoptosis through inhibiting the activity of Bax.

About 940 out of 10,000 miRNAs have been identified as the post-transcriptional regulators of human health-related genes. It is known that different miRNAs in a variety of cells and tissues are biomarkers for the detection of the occurrence and development of diseases, and they also exert therapeutic effects (9). It has been previously reported that miRNAs serve as biomarkers and therapeutic targets for heart failure, players in cardiac remodeling or mediators of transcriptome and proteomic molecules during heart failure. According to previous studies, several miRNAs can be used as key factors controlling the pathophysiological sequelae of acute MI. Therefore, this study was conducted to reveal whether miR-320a plays a role in the treatment of MI through the VEGF signaling pathway. MiRNAs are small non-coding RNAs that bind to complementary sequences on mRNAs and regulate many biological processes. It is known that many miRNAs are involved in the pathophysiology of heart diseases, as well as the repair and regeneration of heart tissues. Recent studies have reported that miRNAs, including miR-15b (14), miR-34a (15), miR-92a (16) and miR-320 (17), are involved in regulating myocardial apoptosis after MI. However, the related regulatory mechanism of miR-320a in myocardial apoptosis after MI has not been reported in detail yet (18,19).

Conclusions

In the present study, the silencing of miR-320a expression in myocardial cells of MI rats raised the expressions of VEGF and Bax, indicating that miR-320a silencing can increase the myocardial apoptosis and the VEGF expression in MI. In conclusion, the results of this study confirm the effect of miR-320a on myocardial apoptosis in MI, which suggests that inhibiting miR-320a facilitates myocardial apoptosis through the VEGF signaling pathway.

Conflict of Interest

The authors declared no conflict of interest.

References

1. Thygesen K, Alpert JS, Jaffe AS, et al. Fourth universal definition of myocardial infarction (2018). Eur Heart J 2019; 40(3): 237-269.
2. Xiang Y, Zhang Z, Xie C, et al. Serum Cat S, TSP-1, IL-11, BNP and sST2 Diagnostic and Prognostic Value in Chronic Heart Failure. Altern Ther Health M 2022; 28(4): 55-59.
3. Inandiklioglu N, Demir V, Celik Y, Demirtas M. Leukocyte telomere length and lipid parameters in patients with myocardial infarction with non-obstructive coronary arteries. Cell Mol Biol 2021; 67(6): 346-352.
4. Guo CX, Jiang X, Zeng XJ, et al. Soluble receptor for advanced glycation end-products protects against ischemia/reperfusion-induced myocardial apoptosis via regulating the ubiquitin proteasome system. Free Radical Bio Med 2016; 94(17-26.
5. Lopes BT, Montrezol FT, Silva Terra VD, Medeiros A. A Single Mindfulness-Based Meditation Session Can Produce Reductions in Cardiovascular Risk in Hypertensive Patients: A Pilot Study. Altern Ther Health M 2022; 28(2): 18-23.
6. Yaseen MS, Ali NAM. The effect of bempedoic acid an ATP-citrate lyase inhibitor on cardiovascular risk factors in rats with experimentally induced myocardial infarction and hyperlipidemia. Cell Mol Biol 2022; 68(10): 94-99.
7. Salimath AS, Phelps EA, Boopathy AV, et al. Dual delivery of

hepatocyte and vascular endothelial growth factors via a protease-degradable hydrogel improves cardiac function in rats. Plos One 2012; 7(11): e50980.
8. Zhang F, Tang Z, Hou X, et al. VEGF-B is dispensable for blood vessel growth but critical for their survival, and VEGF-B targeting inhibits pathological angiogenesis. P Natl Acad Sci Usa 2009; 106(15): 6152-6157.
9. Abid MR, Schoots IG, Spokes KC, Wu SQ, Mawhinney C, Aird WC. Vascular endothelial growth factor-mediated induction of manganese superoxide dismutase occurs through redox-dependent regulation of forkhead and IkappaB/NF-kappaB. J Biol Chem 2004; 279(42): 44030-44038.
10. Wen S, Shao G, Zheng J, Zeng H, Luo J, Gu D. Apatinib regulates the cell proliferation and apoptosis of liver cancer by regulation of VEGFR2/STAT3 signaling. Pathol Res Pract 2019; 215(4): 816-821.
11. Pasquinelli AE. MicroRNAs and their targets: recognition, regulation and an emerging reciprocal relationship. Nat Rev Genet 2012; 13(4): 271-282.
12. Yang L, Ma T, Zhang Y, Wang H, An R. Construction and Analysis of lncRNA-miRNAmRNA ceRNA Network Identify an Eight-Gene Signature as a Potential Prognostic Factor in Kidney Renal Papillary Cell Carcinoma (KIRP). Altern Ther Health M 2022; 28(6): 42-51.
13. Meloni M, Marchetti M, Garner K, et al. Local inhibition of microRNA-24 improves reparative angiogenesis and left ventricle remodeling and function in mice with myocardial infarction. Mol Ther 2013; 21(7): 1390-1402.
14. Liu L, Zhang G, Liang Z, et al. MicroRNA-15b enhances hypoxia/reoxygenation-induced apoptosis of cardiomyocytes via a mitochondrial apoptotic pathway. Apoptosis 2014; 19(1): 19-29.
15. Iekushi K, Seeger F, Assmus B, Zeiher AM, Dimmeler S. Regulation of cardiac microRNAs by bone marrow mononuclear cell therapy in myocardial infarction. Circulation 2012; 125(14): 1765-1773, S1- S7.
16. Hinkel R, Penzkofer D, Zuhlke S, et al. Inhibition of microRNA-92a protects against ischemia/reperfusion injury in a large-animal model. Circulation 2013; 128(10): 1066-1075.
17. Ren XP, Wu J, Wang X, et al. MicroRNA-320 is involved in the regulation of cardiac ischemia/reperfusion injury by targeting heat-shock protein 20. Circulation 2009; 119(17): 2357-2366.
18. Azizi Dargahlou, S., Iriti, M., Pouresmaeil, M., Goh, L. P. W. MicroRNAs; their therapeutic and biomarker properties. Cell Mol Biomed Rep 2023; 3(2): 73-88. doi: 10.55705/cmbr.2022.365396.1085
19. Kanwal, N., Al Samarrai, O., Al-Zaidi, H. M. H., Mirzaei, A., Heidari, M. Comprehensive analysis of microRNA (miRNA) in cancer cells. Cell Mol Biomed Rep 2023; 3(2): 89-97. doi: 10.55705/cmbr.2022.364591.1070.